JOURNAL OF MASS SPECTROMETRY, VOL. 32, 188–200 (1997)

Gas-phase Unimolecular Reactivity of $C_3H_7O^+$ Cations: a Combined Mass Spectrometric–Molecular Orbital Study

G. Bouchoux,[1]* F. Penaud-Berruyer,[2] H. E. Audier,[1] P. Mourgues[1] and J. Tortajada[3]

[1] Laboratoire des Mécanismes Réactionnels, UA CNRS 1307, Ecole Polytechnique, 91128 Palaiseau Cedex, France

[2] Laboratoire de Physicochimie des Rayonnements, UA CNRS 75, Bât. 350, Centre Universitaire Paris-Sud, 91405 Orsay Cedex, France

[3] Laboratoire de Chimie Structurale Organique, Université Pierre et Marie Curie (Paris VI), 4 Place Jussieu, 75252 Paris Cedex 05, France

The unimolecular dissociations of the two isomeric ions $[CH_3CH_2CHOH]^+$ (1) and $[CH_3CH_2OCH_2]^+$ (2) were re-examined. Molecular orbital calculations conducted at the MP2/6–31G*//HF/6–31G* + ZPE level were used to characterize the corresponding potential energy profile. The experimental data were completed by a Fourier transform ion cyclotron resonance spectrometric investigation on the system $[CH_2OH]^+ + C_2H_4$ and by a study of various metastable $[C_3H_7O]^+$ ions. The isomerization pathway of lowest energy connecting 1 and 2 involves two ion–neutral complexes between protonated formaldehyde and ethene. The isomerization $1 \rightleftharpoons 2$ is typically a complex mediated reaction since the key step consists simply of the reorientation of the two partners $[CH_2OH]^+$ and C_2H_4 inside the ion–neutral cage. The model is demonstrated to account for the H–D exchange observed during the dissociation of variously deuterated species. © **1997 by John Wiley & Sons, Ltd.**

J. Mass Spectrom. **32**, 188–200 (1997)
No. of Figures: 4 No. of Tables: 5 No. of Refs: 14

KEYWORDS: $C_3H_7O^+$; dissociation mechanism; ion–neutral complexes; molecular orbital calculation

INTRODUCTION

Unimolecular chemistry of gaseous organic ions is increasingly described in terms of 'weakly coordinated cations',[1] a concept first introduced by Bowen *et al.*[2] in their pioneering work on $[C_3H_8N]^+$ and $[C_3H_7O]^+$ ions. We recently re-investigated the dissociation mechanisms of the former species with the help of molecular orbital calculations and Fourier transform ion cyclotron resonance spectrometry.[3] In the same vein, the aim of the present study was to provide new information, both experimental and theoretical, on the $[C_3H_7O]^+$ system.

Concerning these species, it is well known that the metastable ions $[CH_3CH_2CHOH]^+$ (**1**) and $[CH_3CH_2OCH_2]^+$ (**2**) undergo the same dissociation reactions leading to $[C_3H_5]^+$ and $[CH_2OH]^+$ ions.[2,4–9] Bowen *et al.*[2] proposed that during the dissociation of these ions a C—O bond is stretched and the ion–dipole interactions between the incipient fragments allow the opening of the new reaction channels, less energy demanding than the direct decomposition. The identical behaviour was logically explained by assuming that **1** and **2** interconvert via a weakly coordinated structure in which neutral ethene and neutral formaldehyde are bonded by a proton, $[C_2H_4, H^+, CH_2O]$ (**5**) (Scheme 1). This first study was later completed experimentally by the work of Holmes *et al.*[7] and McAdoo and Hudson[8] and theoretically by a molecular orbital study by Nobes and Radom[10] on several $[C_3H_7O]^+$ ion structures.

Much new information on the isomerization/dissociation of $[C_3H_7O]^+$ ions presented in Scheme 1 is discussed in this paper. First, bimolecular reactions involving the dissociation products of ions **1** and **2** were examined in a Fourier transform ion cyclotron resonance (FT-ICR) mass spectrometer. Additional experimental information was provided by studying the unimolecular decomposition of protonated allyl alcohol and several $[C_3H_7O]^+$ ions produced in the source of ZAB mass spectrometer under chemical ionization conditions. Finally, the reaction pathways depicted in Scheme 1 were considered from a theoretical point of view using MP2/6–31G*//HF/6–31G* + ZPE *ab initio* molecular orbital calculations.

EXPERIMENTAL AND COMPUTATIONAL

Unimolecular dissociation of metastable ions were studied in the second field-free region on a VG ZAB 2F double analyser mass spectrometer working in the mass analysed ion kinetic energy (MIKE) mode. Typical instrument conditions were source temperature 150 °C, accelerating voltage 8 kV and ionizing energy 70 eV. The kinetic energy release values were calculated after correction for the width of the main beam. Collision-

* Correspondence to: G. Bouchoux.

CCC 1076–5174/97/020188–13 $17.50

Received 11 September 1996
Accepted 23 October 1996

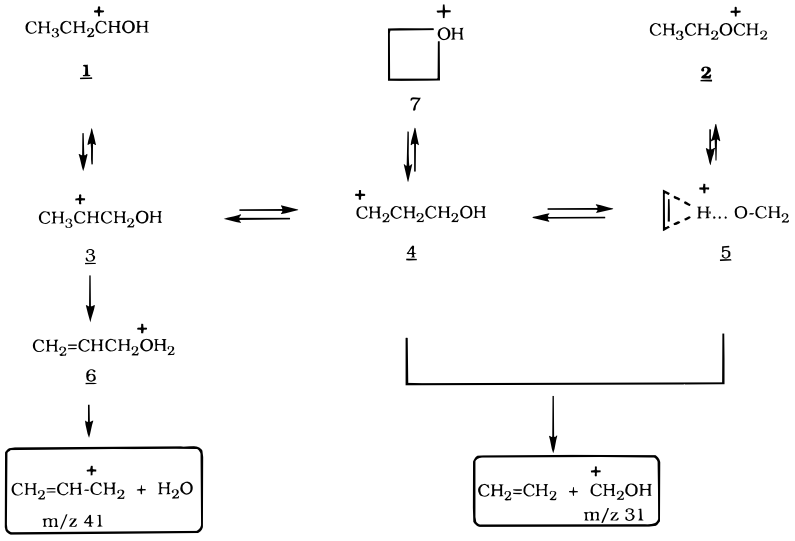

Scheme 1

induced dissociations (CID) were performed using helium as the target gas. Helium was introduced into the collision cell until the precursor ion abundance was suppressed to 75%. Ions $[CH_3CH_2CHOH]^+$ (**1**) and $[CH_3CH_2OCH_2]^+$ (**2**) were generated in the ion source by dissociative ionization of butan-2-ol and ethyl propyl ether, respectively.

Ion–molecule reactions were performed with a Bruker CMS 47X FT-ICR instrument by injecting reactant ions from an external electron impact ion source into a cell containing the neutral reactant at a constant pressure (2×10^{-7} mbar for ethene-d_0 or -d_4, 2×10^{-8} mbar for CH_2O). Unwanted ions were ejected by a combination of chirp and soft r.f. pulses and, unless specified otherwise, the remaining ions were relaxed to thermal energies either by the presence of a static pressure of argon or, in the case of ethene, by the neutral reactant itself. The $[CX_2OH]^+$ ions (X = H, D) were produced by dissociative ionization of the suitably deuterated ethanol in the external source of the FT-ICR spectrometer. Deuteronated ions CX_2OD^+ were produced in a similar way in the presence of D_2O in the inlet system of the external source. Allyl cations were generated by low-energy (20 eV) electron impact on 3-bromopropene.

Ab initio molecular orbital calculations were performed using the Gaussian 92 suites of programs.[11a] The geometries of the different structures (stationary or saddle points) included in this study were fully optimized at the Hartree–Fock level of theory employing suitable gradient methods. These optimizations were carried out using the 6–31G* basis set. The harmonic vibrational frequencies were determined at the same level, by analytical second-derivative calculations and used first to characterize stationary and saddle points of the potential surface and second to evaluate zero-point vibrational energies (ZPE) which were scaled by the empirical factor 0.9.[11b] Improved energy estimations were obtained by including effects of valence electron correlation using second order Møller–Plesset perturbation theory (MP2). Thus, the level of theory discussed within the text refers to MP2/6–31G*//HF/6–31G* + ZPE(HF/6–31G*).

RESULTS AND DISCUSSION

Unimolecular processes studied by tandem mass spectrometry

The unimolecular dissociations of metastable ions **1** and **2** have been previously studied by several workers in the first[2] and in second[7,8] field-free regions (FFR) of the mass spectrometer. Two competitive pathways have been identified: elimination of H_2O (100%, $T_{0.5} = 28$ meV, for both precursors) and loss of C_2H_4 (7%, $T_{0.5} = 23$ meV from **1** and 4%, $T_{0.5} = 20$ meV from **2**). These reactions are preceded by an almost complete exchange of all hydrogen atoms. However, for **1** the hydroxylic position is less affected than the carbon positions by this scrambling; similarly, preferential β-hydrogen transfer seems to precede elimination of both H_2O and C_2H_4 from **2**. Protonated oxetane and protonated allyl alcohol have also been characterized in studies of selected $[C_3H_7O]^+$ ions formed by chemical ionization.[12]

Our own results using the MIKE technique fully confirm most of the data reported by others[2,7,8] (Table 1). Some complementary information must be mentioned.

First, it appears that the lifetime of the ions has no or only a marginal influence on the extent of the hydrogen exchange. For instance, for the isotopomer $[CH_3CH_2CHOD]^+$, the ratio m/z 31/32 (loss of ethene) and the ratio m/z 41/42 (loss of water) is almost constant in the 2nd FFR and the 1st FFR (or when the accelerating voltage is varied between 8 and 3 kV).

Furthermore, the collisionally activated dissociations of cations **1** and **2** are very similar (in particular the ratio m/z 31/41 is almost identical), indicating either a very small barrier for **1** ⇄ **2** isomerization or the sampling of the same mixture of isomers whatever the precursor may be.

We examined the MIKE spectrum of $[C_3H_7O]^+$ ions formed from a mixture of allyl alcohol and H_2O under chemical ionization conditions. This spectrum shows an m/z 31 Gaussian peak and an m/z 41 composite peak.

Table 1. Metastable ion dissociations from $[C_3X_6OX]^+$ and $[C_2X_5OCX_2]^+$ (X = H, D) ions[a]

	Loss of ethylene						Loss of water			
	31	32	33	34	41	42	43	44	45	46
$CH_3CH_2CHOD^+$	**37**	**63**	—	—	**66**	**34**	—	—	—	—
	[29]	[71]	—	—	[67]	[33]	—	—	—	—
	(35)	(65)	—	—	(74)	(26)	—	—	—	—
	86	*14*			*29*	*71*				
$CH_3CH_2CDOH^+$	**57**	**43**	—	—	**12**	88	—	—	—	—
	[59]	[41]	—	—	—	—	—	—	—	—
	(60)	(40)	—	—	(13)	(87)	—	—	—	—
	86	*14*			*29*	*71*				
$CH_3CD_2CHOH^+$	**30**	**57**	**13**	—	**1**	**26**	**73**	—	—	—
	[32]	[55]	[13]	—						
	(28)	(60)	(10)	—	—	(25)	(75)	—	—	—
	29	*57*	*14*		*5*	*48*	*48*			
$CD_3CH_2CHOH^+$	**12**	**53**	**33**	**2**	—	**2**	**34**	**64**	—	—
	[16]	[52]	[32]							
	(20)	(31)	(47)	(2)	—	(2)	(34)	(64)	—	—
	11	*51*	*34*	*3*		*14*	*57*	*29*		
$CH_3CD_2CDOH^+$	**12.5**	**53**	**32.5**	**2**	—	**3**	**38.5**	**55.5**	**3**	—
	11	*51*	*34*	*3*		*14*	*57*	*29*		
$CH_3CH_2OCD_2^+$	**25**	**52**	**22**	—	—	**28**	**72**	—	—	—
	[22]	[51]	[27]	—	[1]	[26]	[73]			
	(26)	(58)	(14)	—	—	(21)	(79)	—	—	—
	29	*57*	*14*		*5*	*48*	*48*			
$CH_3CD_2OCH_2^+$	**26.5**	**56.5**	**17**	—	**2**	**32**	**65**	—	—	—
	[35]	[52]	[13]	—	[1]	[31]	[68]	—	—	—
	(28)	(56)	(16)	—	(2)	(37)	(61)	—	—	—
	29	*57*	*14*		*5*	*48*	*48*			
$CD_3CH_2OCH_2^+$	**7**	**48**	**49**	**3**	—	**9**	**64**	**27**	—	—
	[11]	[52]	[33]	[3]	—	[8]	[65]	[27]	—	—
	11	*51*	*34*	*3*	—	*14*	*57*	*29*		
$CD_3CD_2OCH_2^+$	—	**12.5**	**54**	**33.5**	—	—	—	**34.5**	**62**	**3.5**
		14	*57*	*29*	—	—	—	—	—	—
	—	(14)	(67)	(19)	—	—	—	(70)	(29)	(1)
		14	*57*	*29*	—	—	—	*48*	*48*	*5*

[a] In bold, this work; in square brackets, from Ref. 8; in parentheses, from Ref. 2; italic, statistical distribution assuming total hydrogen scrambling.

Reaction with D_2O gives $[C_3H_5D_2O]^+$ ions whose MIKE spectrum exhibits two kinds of peaks, (i) *m/z* 31, 32 and 33 (losses of $C_2H_2D_2$, C_2H_3D and C_2H_4, respectively) in the ratio 15:63:22 and (ii) *m/z* 41, 42 and 43 (losses of D_2O, HDO and H_2O, respectively) in the ratio 6:70:24. The *m/z* 41 peak is composite with a narrow ($T_{0.5} = 1$ meV) and a large ($T_{0.5} = 24$ meV) Gaussian component; the peaks *m/z* 42 and 43 are simple Gaussian ($T_{0.5} = 25$ meV). Similar observations are made when using CH_4 as reactant gas: the MIKE spectrum of $[C_3H_7O]^+$ ions contains a composite peak for the water loss (*m/z* 41, 60% intensity) and a simple Gaussian peak for the ethene elimination (*m/z* 31, 40% intensity). With CD_4 we observe the formation of ions $[C_3H_6DO]^+$ whose MIKE spectrum presents signals at *m/z* 42 (H_2O loss, simple Gaussian, 70%), *m/z* 41 (HDO loss, composite, 30%), *m/z* 32 (C_2H_4 loss, simple Gaussian, 45%) and *m/z* 31 (C_2H_3D loss, simple Gaussian, 55%). These results compare reasonably well with the data reported by Harrison and co-workers,[12] who studied allyl alcohol under D_2/CI conditions.

Interestingly, the reaction of allyl chloride with D_2O in the ion source of the mass spectrometer under chemical ionization conditions generates $[C_3H_5D_2O]^+$ ions. These ions lose exclusively D_2O in their metastable decompositions with a very small kinetic energy release ($T_{0.5} = 1$ meV) and no ethene elimination is detected. Considering the high propensity of ionized allyl chloride to give allyl cation, the structure of the $[C_3H_5D_2O]^+$ species may be an adduct involving an allyl cation and a molecule of D_2O.

Thus a mixture of $[C_3H_7O]^+$ ions seems to be produced by reactions between allylic compounds and water under high-pressure chemical ionization conditions. One of these structures undergoes a pure water loss with a very low $T_{0.5}$ value and without any prior exchange of the hydrogen atoms between the carbon and the oxygen. The other(s) present the same characteristics as the system **1** ⇄ **2**. It may be suggested that the first structure is a proton bound complex $[C_3H_5{\cdots}D_2O]^+$ or low internal energy protonated allylic alcohol, and that the second is a reaction intermediate involved during the isomerization/dissociation of **1** and **2**.

Bimolecular processes studied by FT-ICR mass spectrometry

Ion–molecule reactions, performed under the FT-ICR conditions described in the Experimental section, allow the exploration of the potential energy surface within

various energy regimes. The two entries first explored are the reactions of the allyl cation with H_2O and of CH_2OH^+ with ethene, which correspond to the two main unimolecular dissociation reactions of ions **1** and **2**. A third possible entry on the potential energy surface was also briefly investigated, namely the reaction of the ethyl cation with neutral formaldehyde. For each case, the reactions occurring within the encounter complexes have been followed by using a set of labelled ions or neutrals.

The reaction of protonated formaldehyde with ethene was thoroughly studied using all the possible CX_2OX^+ ions (X = H, D) and C_2H_4 or C_2D_4 as neutral reactants. Two reactions are observed from the encounter complex, giving rise to CX_3O^+ and $C_3X_5{}^+$ ions, the former reaction being the major process. The set of experiments gives a series of kinetic results presented in Table 2. It first appears that the rate of the reaction ($k_{exp} \approx 10^{-10}$ s^{-1} molecule^{-1} cm^3) is about one order of magnitude lower than the theoretical rate constant derived from the trajectories method of Su and Chesnavitch[13] ($k_{coll} = 1.25 \times 10^{-9}$ s^{-1} molecule^{-1} cm^3). The data reported in Table 2 also seem to indicate that the experimental rate constant is subject to a small to moderate H–D isotope effect. These points are discussed below.

Loss of water. Reaction between CH_2OH^+ ions and C_2H_4 leads to $C_3H_5{}^+$ ions. The use of labelled species shows that this slow reaction is preceded by extensive hydrogen exchanges involving all the positions of the reactants. However, it is difficult to decide to what extent the observations may be described by a statistical distribution of the label because secondary reactions readily consume the allyl cations. For example, the early appearance of $^{13}C^{12}C_2H_5{}^+$ ions (*m/z* 42) during the reaction of $^{13}CD_2OD^+$ ions with ethene demonstrates the occurrence of consecutive reactions leading to a 'dilution' of the deuterium labelling. Similarly, we note the formation of ions of *m/z* 41, $C_3H_5{}^+$, from reactants $CD_2{=}OD^+ + C_2H_4$ and ions of *m/z* 46, $C_3D_5{}^+$, from $CH_2{=}OH^+ + C_2D_4$. The presence of these ions may be attributed to further reactions of $C_3X_5{}^+$ ions with ethene-d_0 or $-d_4$. Indeed, we observe that reaction of the allyl cation with C_2D_4 gives rise to variously exchanged $C_3X_5{}^+$ species. Moreover, this reaction proceeds at nearly collision rate, i.e. more readily than the rate of formation of the allyl cations, thus preventing any interpretative use of the relative abundances of the $C_3X_5{}^+$ ions.

Table 2. Experimental rate constants[a] for reactions $[CX_2OX]^+ + C_2X_4$ (X = H or D)

Reactants	k_{exp} (cm^3 molecule^{-1} s^{-1})
$[CH_2OD]^+ + C_2H_4$	1.14×10^{-10}
$[CD_2OH]^+ + C_2D_4$	0.80×10^{-10}
$[CD_2OH]^+ + C_2H_4$	0.77×10^{-10}
$[CH_2OD]^+ + C_2D_4$	0.86×10^{-10}
$[CD_2OD]^+ + C_2H_4$	1.37×10^{-10}
$[CH_2OH]^+ + C_2D_4$	1.20×10^{-10}

[a] Total rate of disappearance of the $[CX_2OX]^+$ species.

Back-reaction to protonated formaldehyde. Although only a few conclusions can be drawn from the previous reaction channel, the back-dissociation to protonated formaldehyde and ethene, in contrast, provides interesting information. The formation of CX_3O^+ ions (*m/z* 31–34) is the major process observed. The reactions of various labelled reactants clearly demonstrate the occurrence of hydrogen atom exchanges which are faster than the back-reaction to protonated formaldehyde. For instance, CH_2OD^+ ions react rapidly with ethene to give CH_2OH^+ ions, showing that the encounter complex returns back to the original structure after hydrogen exchanges involving the hydroxylic position:

$$CH_2OD^+ + CH_2{=}CH_2 \rightarrow CH_2OH^+ + CHD{=}CH_2$$

Complementary information is given by the observation of the reaction

$$CD_2OH^+ + CD_2{=}CD_2 \rightarrow CD_2OD^+ + CHD{=}CD_2$$

Exchange also occurs with the methene part of protonated formaldehyde. This is shown, for example, by the appearance of signals at *m/z* 32 and 31 with reactants $CD_2OH^+ + C_2H_4$; a similar situation arises for the reactions $CD_2OD^+ + C_2H_4$, $CH_2OH^+ + C_2D_4$ and $CH_2OD^+ + C_2D_4$ (Table 3). In fact, in order to explain the results, hydrogen exchanges involving both hydroxyl and methene positions should be considered. In addition, care should be taken regarding the occurrence of consecutive reactions that complicate the situation.

In Table 3, the distribution of the label in the CX_3O^+ ions is compared with statistical models involving (i) only the six C-bonded hydrogen atoms (model A), (ii) the seven hydrogen atoms of the system (model B) and (iii) 55% of model B plus 45% of a srambling involving the hydroxylic hydrogen and the ethene molecule (model C). In all cases the presence of the bulk of parent ions prevents us from obtaining the complete H–D distribution. However, it appears that neither model A nor B may account correctly for the experimental results. A satisfactory agreement is only obtained with model C. This observation points to a scrambling process in which two distinct pathways are operating, one involving the hydroxylic hydrogen and the other the methene group.

The difference in behaviour between the hydroxylic hydrogen and the CH_2 moiety is also reflected by the rate constant values in Table 2. The main observation is that the H–D exchanges are slower for the methene hydrogen than for the hydroxylic hydrogen. For example, the rate of disappearance of CH_2OD^+ with C_2H_4 (or CH_2OH^+ with C_2D_4) is ~1.5 times faster than the reactions involving the CH_2 alone (i.e. $CD_2OH^+ + C_2H_4$ or $CH_2OD^+ + C_2D_4$, see Table 2). Also worth noting is the existence of an isotope effect, *i*, during this hydrogen exchange: compare the rate constants for reactions $CH_2OD^+ + C_2H_4$ and $CD_2OH^+ + C_2D_4$ ($i = 1.4$) and $CD_2OD^+ + C_2H_4$ and $CH_2OH^+ + C_2D_4$ ($i = 1.14$).

Finally, an important point to be emphasized is the formation of ~5% of $^{12}CH_2OH^+$ ions at $t = 1.5$ s when using the reactants $^{13}CH_2OH^+ + CH_2{=}CH_2$. Hence there is a minor process in which the carbon atoms are also exchanged.

Table 3. Relative abundances of $[CX_2OX]^+$ (X = H or D) ions after reaction with ethene (reaction time = 0.5 s; pressure = 2×10^{-7} mbar)

		m/z[b]			
Reactants	Model[a]	31 $[CH_3O]^+$	32 $[CH_2DO]^+$	33 $[CHD_2O]^+$	34 $[CD_3O]^+$
$C_2H_4 + CD_2OH +$		49	51	*	
	A	[57]	[43]	*	
	B	[33]	[67]	*	
	C	[33]	[67]	*	
$C_2H_4 + CD_2OD +$		13	19	68	*
	A	[0]	[43]	[57]	*
	B	[12]	[53]	[35]	*
	C	[7]	[29]	[64]	*
$C_2D_4 + CH_2OH +$		*	59	31	10
	A	*	[57]	[43]	[0]
	B	*	[35]	[53]	[12]
	C	*	[64]	[29]	[7]
$C_2D_4 + CH_2OD +$			*	61	39
	A		*	[57]	[43]
	B		*	[67]	[33]
	C		*	[67]	[33]

[a] (A) model assuming that the hydroxylic hydrogen remains in its position; the hydrogen scrambling involves only six H–D; (B) total hydrogen scrambling, seven H–D; (C) scrambling involving 45% only ethene and the hydroxylic H and 55% total hydrogen scrambling.
[b] Asterisks indicate parent ion.

Reaction of ethyl cation with CH_2O. We also briefly studied the ion–molecule reaction of $C_2H_5^+$ ions with neutral formaldehyde, which is a third possible entry to the system under study, albeit with more initial internal energy. In this case, as expected from the relative proton affinities of ethene and formaldehyde (680 and 720 kJ mol^{-1}, respectively), the only reaction observed is the protonation of formaldehyde, which occurs nearly at collision rate.

Furthermore, when $C_2D_5^+$ is allowed to react with CH_2O, the D^+ transfer is fast enough to prevent any H–D exchange from occurring and, consequently, this reaction was not investigated further.

Reaction of the allyl cation with D_2O. The last possible entry in the present system corresponds to the reactant couple $C_3H_5^+$ plus H_2O; these two species appear during metastable dissociations of both **1** and **2** and in the ion–molecule reaction of CH_2OH^+ with C_2H_4. Starting with $C_3H_5^+$ and D_2O, no significant evolution of the signal at *m/z* 41 is observed even at long reaction times. Therefore, one has to conclude that the allyl cation suffers no hydrogen exchange with water. This useful result will be discussed in the last part of the paper.

Molecular orbital calculations

The previous study of $[C_3H_7O]^+$ ions by Nobes and Radom[10] include HF/3–21G optimized structures and MP3/6–31G*//3–21G energies which have been estimated by additivity. The present investigation was performed at the unified MP2/6–31G*//HF/6–31G* + ZPE level in order (i) to eliminate the possible deficiencies of the limited 3–21G basis set during the optimization of ionic species and (ii) to explore structures involved in Scheme 1 but not previously considered by Nobes and Radom. Figure 1 displays the geometrical parameters of the various equilibrium and transition structures optimized at the HF/6–31G* level for the purpose of this work. Corresponding total and relative energies are recorded in Tables 4 and 5.

Stable covalent structures. As already observed using the 3–21G basis set,[5] both ions $[CH_3CH_2CHOH]^+$ (**1**) and $[CH_3CH_2OCH_2]^+$ (**2**) are found to be more stable in their *syn* conformation at the MP2/6–31G*//HF/6–31G* + ZPE level. Structure **1** is calculated to lie 48 kJ mol^{-1} in energy below structure **2**, a value which agrees well with the experimental enthalpy difference of 43 kJ mol^{-1} deduced from $\Delta H°(\mathbf{1}) = 550$ kJ mol^{-1} and $\Delta H°(\mathbf{2}) = 593$ kJ mol^{-1}.[14]

The secondary cation $[CH_3CHCH_2OH]^+$ (**3**) is a local minimum on the energy surface at the 6–31G* level in its *syn* conformation and for the conformation of the methyl group in which an hyperconjugative effect operates between one of the C—H bonds and the empty p orbital of C(2) (Fig. 1). Nobes and Radom[10] found at the 3–21G level that **3** is stable only if the C_s symmetry is imposed; moreover, they suggested that structure **3** collapses without critical energy to cation **1** by a 1,2-hydride shift; however, they did not pursue this point further. We agree with this suggestion and, in fact, at the 6–31G* level, the transition state **TS1–3** is located 13 kJ mol^{-1} above **3**. However, when correlation effects are introduced, this transition structure becomes more stable than **3** by no less than 41 kJ mol^{-1}! This phenomenon reflects some 'metastable' character of cation **3**, i.e. its existence in a very shallow potential energy well for only few conformations (at least in that indicated in Fig. 1).

Various conformations of the primary cation $[CH_2CH_2CH_2OH]^+$ (**4**) have been investigated. Different attempts to optimize these structures without symmetry constraint give rise to protonated oxetane **7**, to corner protonated cyclopropanol $[CH_2CH_2CH_2(OH)]^+$ (**8**) or to the secondary cation (**3**). Our observations are consistent with those of Nobes

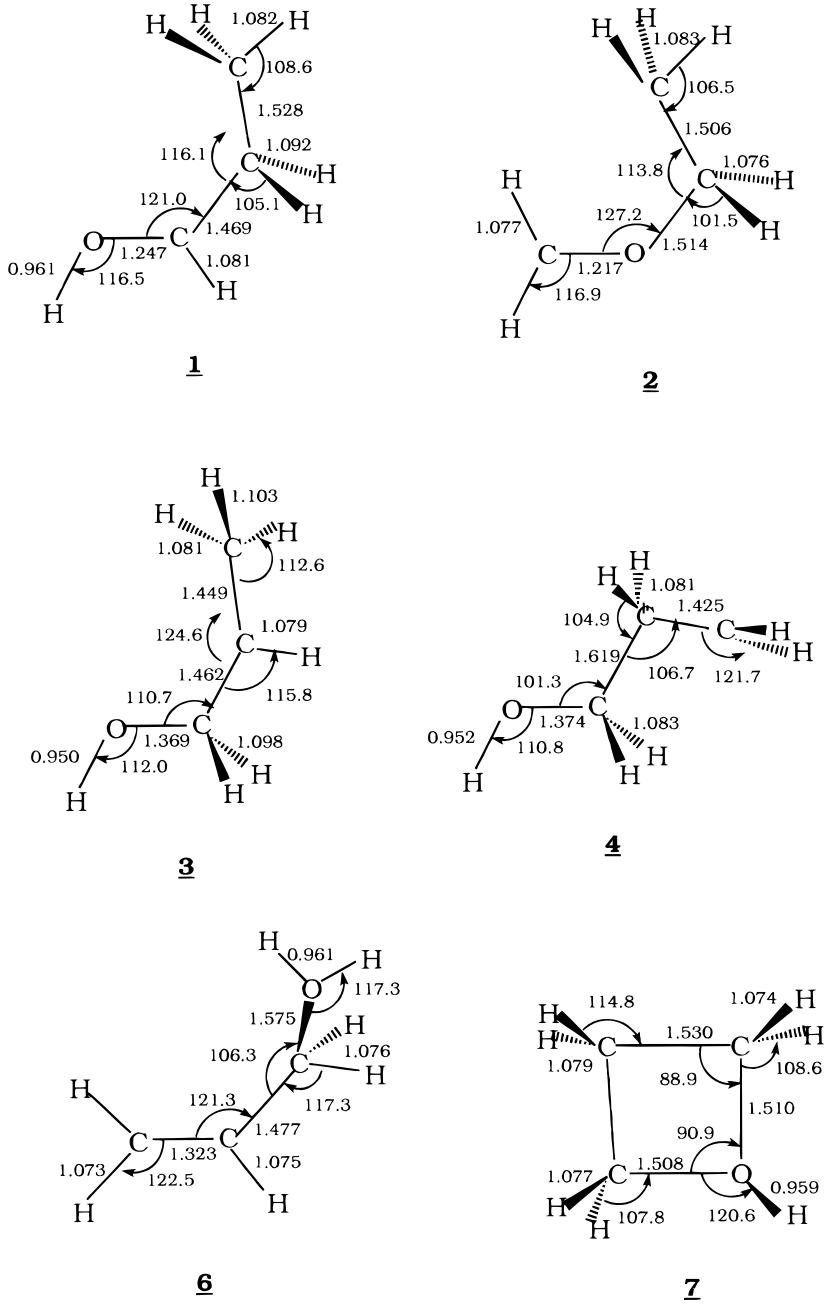

Figure 1. Optimized geometries of $[C_3H_7O]^+$ ions (HF/6–31G*, bond lengths in Å, bond angles in degrees).

and Radom,[10] who suggest also that no activation energy would be expected for the 1,2-hydride shift converting $[CH_2CH_2CH_2OH]^+$ (**4**) to $[CH_3CHCH_2OH]^+$ (**3**). When the C_s symmetry constraint is imposed during the optimization procedure, only the conformation **4b-*anti*** is found to be a local minimum. The C_s symmetry imposed conformations **4a-*syn*** and **4a-*anti*** are characterized by a negative eigenvalue of their force constant matrix corresponding to the torsion around the terminal C—C bond and by relative energies of 253 and 214 kJ mol^{-1}, respectively. The instability of primary cation $[CH_2CH_2CH_2OH]^+$ (**4**) should be compared with the results obtained on the homologous $[CH_2CH_2CH_2NH_2]^+$ cation, for which similar conclusions have been drawn.

Protonated allyl alcohol (**6**) and protonated oxetane (**7**) are predicted to be stable species. Their calculated relative energies with respect to **1** are 74 and 66 kJ mol^{-1}, respectively. These values compare well with the corresponding enthalpy differences of ~66 kJ mol^{-1} for **6** (using a proton affinity value of 790 kJ mol^{-1} for the allyl alcohol) and 75 kJ mol^{-1} for **7**.[14]

The dissociation products $[CH_2CHCH_2]^+ + H_2O$ (**11**) and $[CH_2OH]^+ + C_2H_4$ (**12**) have also been considered. Their calculated energies, relative to **1**, agree reasonably well with the experimental 300 K enthalpy difference (Table 5).

Ion–neutral complexes. The reaction scheme proposed to account for the experimental observations mentioned above is based on the isomerization processes which involve classical hydride or proton migrations and ion–neutral complexes. Several structures may be postulated for the latter; we have investigated by calculation all the

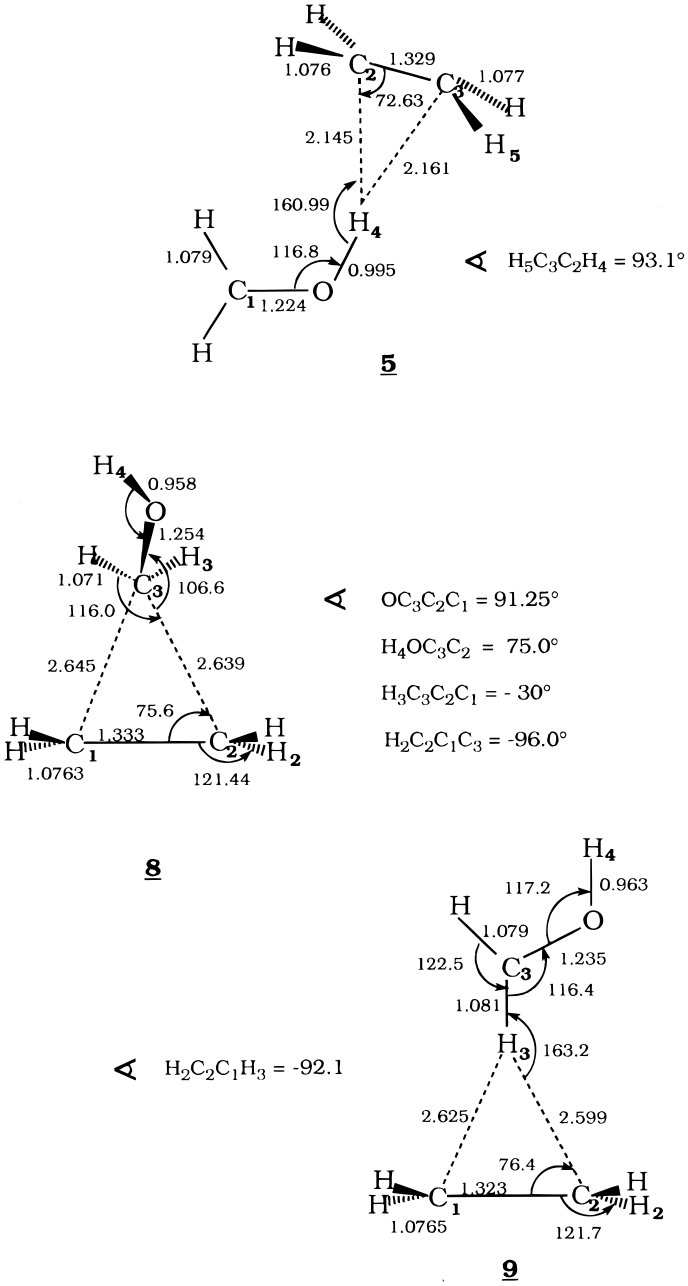

Figure 1. Continued

possible non-covalent structures corresponding to associations between (i) $C_2H_4 + [CH_2OH]^+$ and (ii) $[C_2H_5]^+ + CH_2O$.

For species resulting from interaction between C_2H_4 and $[CH_2OH]^+$, three structures, **5**, **8** and **9**, have been located as minima in the potential energy surface. They correspond to ion–neutral complexes taking their stability from the interaction of either the hydrogen or the carbon atoms of the ionic species $[CH_2OH]^+$ with the π electron system of the ethene molecule. The calculated relative energies of **5**, **8** and **9**, compared with **1**, are 137, 152 and 183 kJ mol^{-1}, respectively. The binding energies of these complexes relative to their separated components ($[CH_2OH]^+CH_2{=}CH_2$) are 75, 60 and 29 kJ mol^{-1}, respectively. Note that structure **8** has been previously located by Nobes and Radom[10] during the search for a stable structure of the primary carbocation **4** using the 3–21G basis set of atomic orbitals. This structure was identified to resemble a loose complex between protonated formaldehyde and ethene. We observe identical structural characteristics when using the 6–31G* basis set (Fig. 1). Structure **9** has been found in a potential energy well only for the *anti* conformation of the hydroxylic hydrogen as indicated in Fig. 1. All attempts of geometry optimization for the *syn* conformation lead to the more stable complex **5**, suggesting that no critical energy is associated with the reaction ***9-syn*** → **5**. However, starting from ***9-anti*** a critical energy of ~100 kJ mol^{-1} is calculated for the rotation of the hydroxyl group along the C—O bond (**TS9-*anti*/9-*syn***).

Concerning the species formed by the interaction of the ethyl cation with formaldehyde, no stable structure can be found at the 6–31G* level of theory. All attempts to optimize such structures lead to **5**. A similar result is obtained when considering the ethyl cation and the

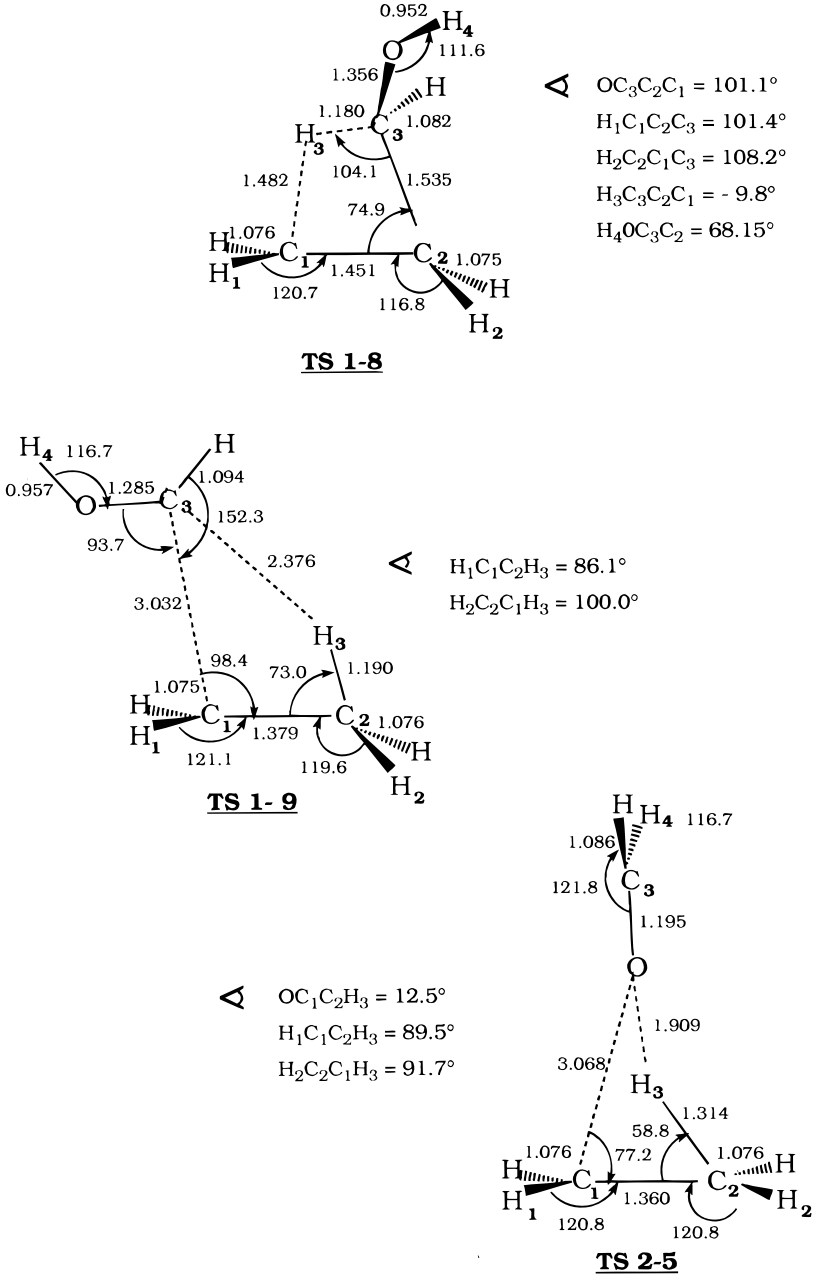

Figure 1. Continued

hydroxycarbene HCOH; only structure **9** is located as a minimum on the energy surface. These results illustrate again the fact that when two species of different proton affinities compete for a proton, only one proton-bonded complex is predicted by the calculation to lie in a tangible energy well. Nevertheless, an interesting feature is that structures corresponding to loosely bonded ethyl cation and neutral (H_2, C, O) species have been located as transition states connecting covalent structures **1** or **2** with **9** or **5**, as will now be discussed.

Transition structures. All the isomerization processes depicted in Scheme 1 were investigated by molecular orbital calculations. The resulting 6–31G* geometries (**TS*i–j***) are displayed in Fig. 1.

Elimination of ethene from either **1** or **2** is, formally, a 1,2-elimination reaction. A number of ion–neutral complexes such as **5** or **9** have been proposed as reaction intermediates during 1,2-elimination reactions of cationic species. In the same vein we investigated the two possible elimination processes expected to lead to ethene loss: $\mathbf{2} \rightarrow \mathbf{5} \rightarrow [CH_2OH]^+ + C_2H_4$ and $\mathbf{1} \rightarrow \mathbf{9} \rightarrow [CH_2OH]^+ + C_2H_4$.

The transition state **TS2–5** is characterized by a structure which looks like a complex between the proton bridged ethyl cation and a molecule of formaldehyde. This result suggests that the structure [CH_2O $CH_3CH_2^+$] postulated by McAdoo and Hudson[8] (Scheme 1) is in fact the transition state **TS2–5**. This transition structure lies 96 kJ mol^{-1} below the dissociation products (**FS3**, $CH_2O + C_2H_5^+$) and 58 kJ mol^{-1} below the final state **FS2** $CH_2OH^+CH_2{=}CH_2$. Another significant result provided by the calculations is the low energy difference between **TS2–5** and the complex **5** itself; this difference amounts for 17 kJ mol^{-1} at the MP2/6–31G*//6–31G* + ZPE level.

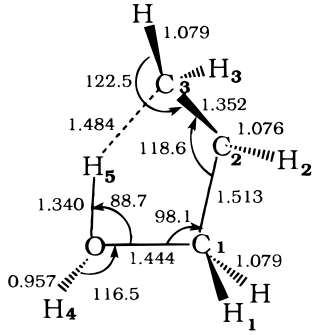

$C_3C_2C_1O = 39.6°$
$H_1C_1C_2C_3 = 156.9°$
$H_2C_2C_1O = -127.8°$
$H_3C_3C_2C_1 = -166.7°$
$H_4OC_1C_2 = 137.4°$
$H_5OC_1C_2 = 2.8°$

TS 3-6

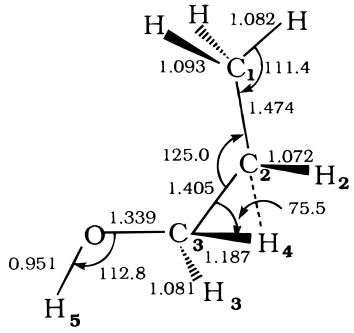

$H_50C_3C_2 = 177°$
$H_3C_3C_2C_1 = -164.6°$
$H_4C_3C_2C_1 = 97.1°$
$H_2C_2C_3O = 173.6°$
$OC_3C_2C_1 = 11.7°$

TS 1-3

Figure 1. Continued

The transition state **TS1–9** possesses a structure resembling a complex between neutral hydroxycarbene and a $C_2H_5^+$ cation distorted from its equilibrium geometry (Fig. 1). Its energy is considerably higher than that of **1** (411 kJ mol^{-1}); nevertheless, the binding energy between proton-bridged $[C_2H_5]^+$ cation and HC—OH is 99 kJ mol^{-1}. The large difference in energy between CH_2O and HC–OH (the latter is 260 kJ mol^{-1} less stable than the former) is in fact reflected by the difference in energy between the transition states **TS1–9**

Table 4. Calculated total energies (hartree) of the investigated $[C_3H_7O]^+$ structures

Structure	HF/3–21G	HF/6–31G*	MP2/6–31G*//HF/3–21G	MP2/6–31G*//HF/6–31G*	ZPVE (6–31G*)[a] (kJ mol^{-1})
1	−191.193 191	−192.265 792	−192.812 660	−192.813 172	244
2	−191.181 435	−192.248 434	−192.794 577	−192.794 841	244
3	−191.155 071	−192.225 962	−192.765 598	−192.765 438	235
4	−191.124 813	−192.191 342	−192.731 920	−192.731 521	238
5	−191.142 289	−192.211 913	−192.758 123	−192.757 593	235
6	−191.189 265	−192.232 386	−192.781 670	−192.784 972	244
7	−191.190 486	−192.238 675	−192.782 820	−192.790 522	251
8	−191.138 972	−192.206 747	−192.756 083	−192.753 016	238
9	−191.127 818	−192.199 095	−192.739 761	−192.739 825	234
10		−192.228 274		−192.766 773	236
TS1–3	−191.139 200	−192.220 771	−192.770 012	−192.768 093	234
TS3–4	−191.118 369		−192.743 929	—	—
TS3–6	−191.122 130	−192.171 786	−192.736 612	−192.740 520	230
TS1–9	−191.042 415	−192.118 659	−192.641 557	−192.648 739	223
TS2–5	−191.127 599	−192.202 509	−192.740 749	−192.746 904	224
TS1–8		−192.191 793		−192.748 831	239
TS9-*anti*/9-*syn*		−192.161 035		−192.698 576	223
FS1	−191.128 08	−192.203 950	−192.739 280	−192.738 970	225
FS2	−191.115 130	−192.188 144	−192.726 710	−192.727 182	230

[a] Zero-point vibrational energies, scaled by a factor of 0.9.

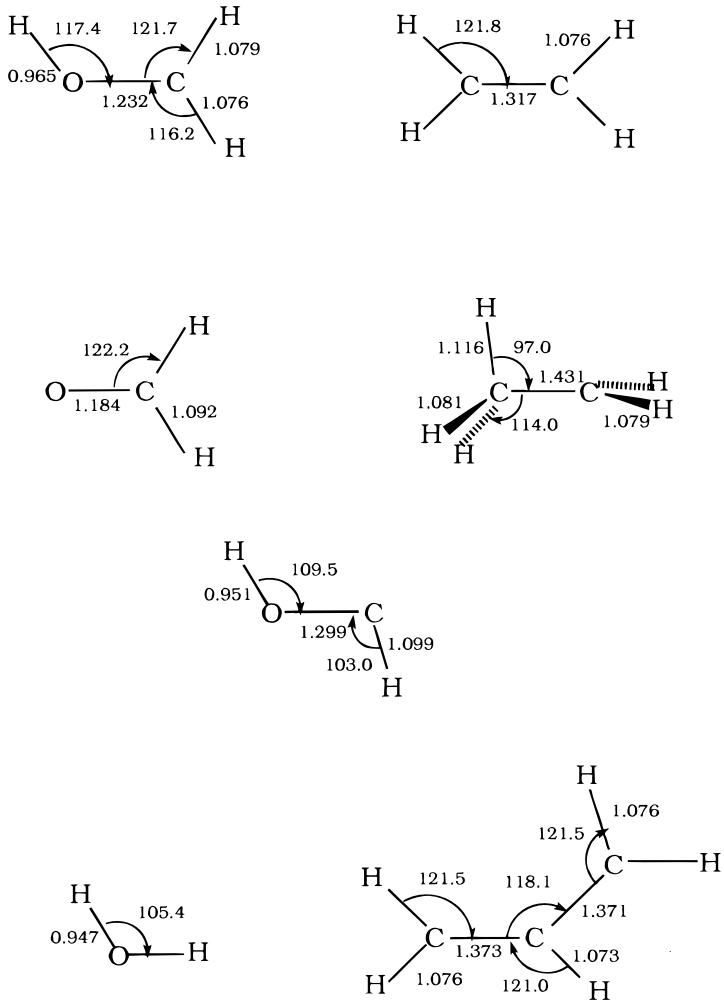

Figure 1. Continued

Table 5. Calculated relative energies (kJ mol^{-1}) of $[C_3H_7O]^+$ ions

Structure	HF/3–21G	HF/6–31G*	MP2/6–31G*//HF/3–21G	MP2/6–31G*//HF/6–31G*	MP2/6–31G*//HF/6–31G* + ZPVE	$\Delta H_{f\,exp}$ (kJ mol^{-1})[a]
1	0	0	0	0	0	0 (550)
2	31	46	48	48	48	43 (593)
3	100	105	124	125	116	—
4	180	195	212	214	208	—
5	134	141	144	146	137	—
6	11	88	82	74	74	75 (625)
7	8	71	79	59	66	66 (616)
8	142	158	149	158	152	—
9	172	175	192	193	183	—
10	—	—	98	—	122	—
TS1–3	142	118	112	85	75	—
TS3–4	197	—	200	—	—	—
TS3–6	187	247	200	191	177	—
TS1–9	396	386	450	432	411	—
TS8–1	—	194	—	169	164	—
TS2–5	174	166	189	174	154	—
TS9-*anti*/9-*syn*	—	275	—	301	280	—
FS1	171	162	193	195	176	158 (708)
FS2	205	204	226	226	212	222 (772)

[a] Experimental 298 K heats of formation (from Ref. 14) are given in parentheses.

and **TS2–5** (257 kJ mol^{-1}). The high critical energy for **9** → **1** and for **9-*anti*** → **9-*syn*** (see above) exclude the participation of both processes during the overall isomerization/dissociation process of **1** and **2**.

The transition states for 1,2-hydride shifts **1** → **3** and **3** → **4** have been discussed in the part devoted to the description of the covalent $[C_3H_7O]^+$ structures **1**, **3** and **4**. It has been suggested that these transition states are best represented by structures **3** and **4** themselves in a convenient conformation. This hypothesis will be made in the elaboration of the potential energy profile associated with Scheme 1.

The transition state for the 1,4-hydrogen migration, **TS3–6**, is situated 103 kJ mol^{-1} above protonated allylic alcohol **6**. This places the transition structure **TS3–6** at the same energy level as the most stable dissociation products: $[CH_2CHCH_2]^+ + H_2O$.

Finally, isomerization reactions involving complex **8** have been considered. First, for the ring-opening/ring-closure process **8** → **7** for which a transition state has been located (**TS7–8**), its energy is only 21 kJ mol^{-1} higher than that of complex **8** and it consequently constitutes an easy process. A second possible reaction from **8** is a concerted 1,2-hydride shift–ring opening leading to **1**. The transition structure **TS1–8** indeed has been located, and it is situated only 12 kJ mol^{-1} above **8**. Finally, attention has been paid to the possible interconversions between complexes **8** and **5**. As long as this process involves only a mutual reorientation of the two partners C_2H_4 and $[CH_2OH]^+$, it is expected that the possible transition state is still stabilized by electrostatic forces and thus lies well below the energy level corresponding to the separated fragments. Unfortunately, the flatness of the potential energy surface in the vicinity of complexes **5** and **8** renders the precise location of transition structures difficult. A higher limit of 20 kJ mol^{-1} may be assigned to the reorientation barrier **8** → **5** by considering the fact that the reaction **8** → **7** is only a marginal process (see later).

Potential energy profile and reaction mechanisms

An isomerization/dissociation mechanism of ions **1** and **2** taking into account the present experimental and theoretical data is proposed in Scheme 2. The corresponding potential energy profile is drawn in Fig. 2.

Isomerization of $[CH_3CH_2CHOH]^+$ (1). The isomerization of protonated propionaldehyde (**1**) into the ion–neutral complex **8** is predicted to occur directly by a concerted process. The transition structure is characterized by a quasi-complete transfer of the migrating hydrogen on the carbon C(1) (C(1)—H = 1.18 Å), thus pointing to an asynchronous process. This proposal differs from the previously suggested mechanism which involved the intermediacy of the primary cation **4** but it is in good agreement with the experimental observations.[2,7,8]

The energy of the transition structure **TS1–8** is significantly below that of both dissociation products, and therefore the reaction **1** ⇌ **8** is reversible. This reversibility may explain the observation of a hydrogen exchange process involving all the C-bonded hydrogen atoms. This result cannot be accounted for by the pathway **1** ⇌ **3** ⇌ **4** since **4** is too high in energy to allow any reversibility before dissociation; this is especially true for the water loss.

Isomerization of $[CH_3CH_2OCH_2]^+$ (2). The isomerization **2** ⇌ **5** occurs via a concerted but asynchronous process. The transition structure looks like a complex between a bridged ethyl cation and neutral formaldehyde: the C(1)—O bond is almost broken whereas the O—H bond remains to be formed. The small difference in energy between **5** and **TS2–5** allows a rapid isomerization **2** ⇌ **5** and thus the complete interchange of the hydrogen atoms of the ethyl chain in metastable ions **1** as well as the hydrogen exchanges observed during the ICR experiments.

O-bonded hydrogen exchange. The participation of the hydroxylic hydrogen in the hydrogen exchange in metastable ions **1** can be explained either by a reversible isomerization between cation **3** and protonated allyl alcohol **6** or by the interconversion **1** ⇌ **2** via the ion–neutral complexes **5** and **8**. The calculation demonstrates that dissociation of **6** into $[C_3H_5]^+ + H_2O$ and its isomerization into **1** require almost the same energy (Fig. 2). Since this competition occurs between a simple cleavage and a rearrangement process, the former reaction is certainly favoured over the latter. This conclusion is corroborated by experiment. Labelled ions **6**, $[CH_2CHCH_2OD_2]^+$, generated by reaction of allyl bromide with D_2O the ion source, exclusively eliminate

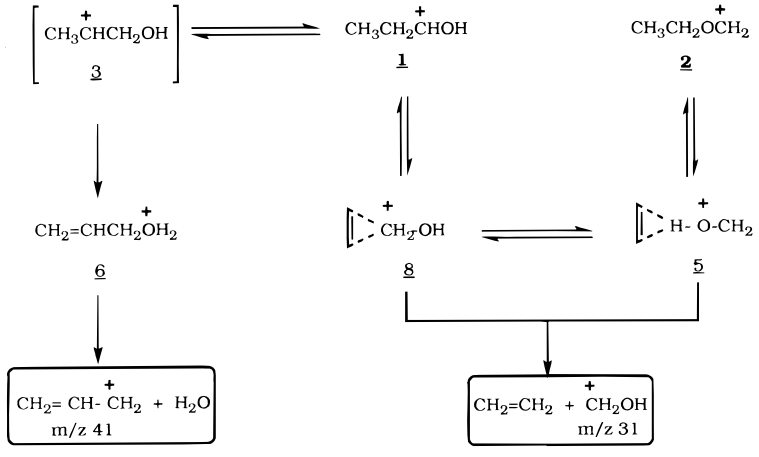

Scheme 2

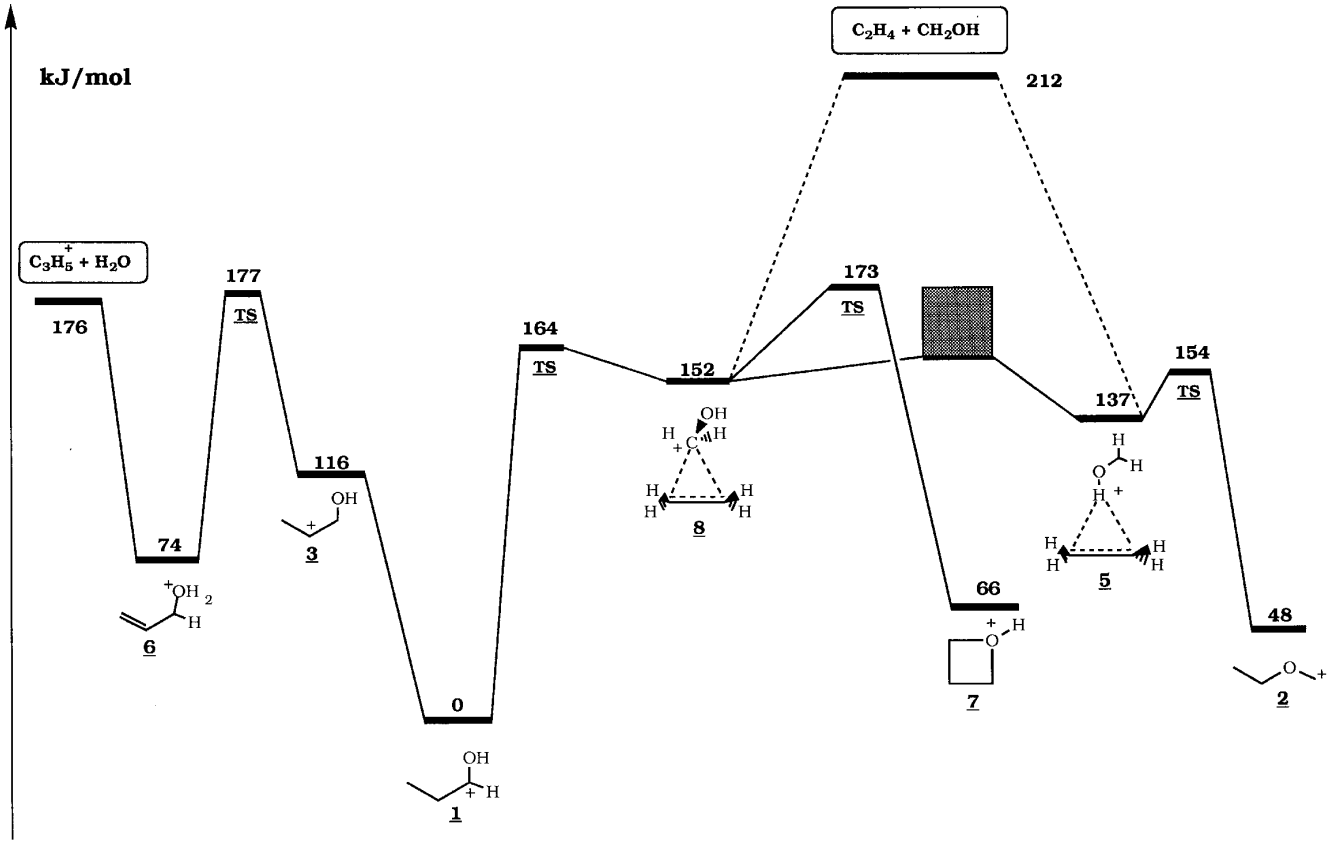

Figure 2. Schematic potential energy diagram for isomerization/dissociation of ions $[CH_3CH_2CHOH]^+$ (**1**) and $[CH_3CH_2OCH_2]^+$ (**2**) (MP2/6–31G*//HF/6–31G* + ZPE results).

D_2O in the 2nd FFR of the ZAB mass spectrometer. Similarly, the absence of H–D exchange between the allyl cation and D_2O noted during the ICR experiments, indicates that the reaction **6** → **3** is not occurring. The part of the potential energy surface explored when starting from the $C_3H_5^+ + H_2O$ reactants is limited to protonated allyl alcohol **6** (or eventually $C_3H_5^+$–H_2O ion–neutral complexes).

Therefore, the reaction **1** ⇌ **3** → **6** is irreversible and the participation of the hydroxylic hydrogen to the exchange must be attributed to the isomerization **1** ⇌ **2**. However, it must be noted that this participation is not complete for metastable ions **1**. This may be due to the comparable critical energy (and frequency factors) values for the isomerization **1** ⇌ **8** ⇌ **5** ⇌ **2** and dissociation **1** ⇌ **3** ⇌ **6** → $[C_3H_5]^+ + H_2O$. The ICR result indicating that the OH and CH_2 hydrogen atoms do not exchange at the same rate, along with the distribution of labelled ions presented in Table 3, is also consistent with the fact that no fast interconversion occurs between complex **8** (responsible for the CH_2 exchanges) and complex **5** (at the origin of the OH exchange).

Intermediacy of protonated oxetane. Protonated oxetane (**7**) is a stable species and the calculation indicates that the transition structure for isomerization **7** → **8** is only 21 kJ mol^{-1} above **8**. Therefore, this reaction may intervene before dissociations of both **1** and **2**. The ICR experiments demonstrate that structure **7** is only marginaly involved.[9a] This limited participation may be explained by the fact that (i) the critical energy for the reaction **8** → **1** is lower than that of the reaction **8** → **7** and (ii) the rearrangement **8** ⇌ **7** involves a ring-closure/ring-opening process for which the frequency factor must be lower than that corresponding to the ion neutral isomerization step **8** ⇌ **5**.

CONCLUSION

The most outstanding result of the present study is that the isomerization pathway of lowest energy connecting $[CH_3CH_2CHOH]^+$ (**1**) and $[CH_3CH_2OCH_2]^+$ (**2**) involves ion–neutral complexes $[CH_2OH\cdots C_2H_4]^+$ (**5** and **8**). The isomerization **1** ⇌ **2** is typically a complex-mediated reaction since the key step **5** ⇌ **8** consists simply in the reorientation of the two partners $[CH_2OH]^+$ and C_2H_4 inside the ion–neutral cage. The two reactions **1** → **8** and **2** → **5** involve a hydrogen migration concerted with an adjacent carbon–carbon or carbon–oxygen bond elongation. This is consistent with the experimental observation of extensive hydrogen scrambling prior to dissociation: all the hydrogen atoms become equivalent after a complete cycle of reactions **1** ⇌ **8** ⇌ **5** ⇌ **2**. Isomerization **8** ⇌ **9** may also participate to the hydrogen and carbon exchange.

The loss of H_2O, the dominant fragmentation of ions **1** and **2**, occurs via the singular structure **3** and protonated allyl alcohol **6**. During this process, the rate determining step is the 1,4-hydrogen migration **3** → **6**.

Elimination of an ethene molecule may occur from one of the various reaction intermediates **5**, **8** and **7** or through the singular structures **3** → **4** by successive 1,2-hydrogen migrations.

REFERENCES

1. For recent reviews, see (a) P. Longevialle, *Mass Spectrom. Rev*. **11**, 157 (1992); (b) D. J. McAdoo and T. H. Morton, *Acc. Chem. Res*. **26**, 295 (1992); (c) R. D. Brown, *Org. Mass Spectrom*. **28**, 1577 (1993).
2. R. D. Bowen, D. H. Williams, G. Hvistendahl and J. R. Kalman, *Org. Mass Spectrom*. **13**, 721 (1978).
3. G. Bouchoux, F. Penaud-Berruyer and J. Tortajada, *Org. Mass Spectrom*. **30**, 723 (1995).
4. G. Hvistendahl and D. H. Williams, *J. Am. Chem. Soc*. **97**, 3097 (1975).
5. D. H. Williams and R. D. Bowen, *J. Am. Chem. Soc*. **99**, 3192 (1977).
6. R. D. Bowen, J. R. Kalman and D. H. Williams, *J. Am. Chem. Soc*. **99**, 5481 (1977).
7. J. L. Holmes, R. T. Rye and J. K. Terlouw, *Org. Mass Spectrom*. **14**, 606 (1979).
8. D. J. McAdoo and C. E. Hudson, *Int. J. Mass Spectrom. Ion Processes* **88**, 133 (1989).
9. (a) J. Tortajada, H. E. Audier, C. Monteiro and P. Mourgues, *Org. Mass Spectrom*. **26**, 913 (1991); (b) G. Bouchoux, F. Penaud-Berruyer, H. E. Audier, P. Mourgues, J. Tortajada, in *Proceedings of the 42nd ASMS Conference on Mass Spectrometry and Allied Topics*, Chicago, IL, 1994, p. 829.
10. R. H. Nobes and L. Radom, *Org. Mass Spectrom*. **19**, 385 (1984).
11. (a) M. J. Frisch, G. W. Trucks, M. Head-Gordon, P. M. W. Gill, M. W. Wong, J. B. Foresman, B. G. Johnson, H. B. Schlegel, M. A. Robb, E. S. Replogle, R. Gomperts, J. L. Andres, K. Raghavachari, J. S. Binkley, C. Gonzalez, R. L. Martin, D. J. Fox, D. J. Defrees, J. Baker, J. J. P. Stewart and J. A. Pople, *Gaussian 92*. Gaussian, Pittsburgh, PA (1991); (b) J. A. Pople, R. Krishnan, H. B. Schlegel and J. S. Binkley, *Int. J. Quantum Chem. Symp*. **13**, 225 (1979).
12. (a) R. D. Bowen and A. G. Harrison, *Org. Mass Spectrom*. **16**, 159 (1981); (b) A. G. Harrison, T. Gaumann and D. Stahl, *Org. Mass Spectrom*. **18**, 517 (1983).
13. T. Su and Chesnavitch,
14. S. G. Lias, J. E. Bartmess, J. F. Liebman, J. L. Holmes, R. D. Levin and W. G. Mallard, *J. Phys. Chem. Ref. Data* **17**, Suppl. 1 (1988).

